Supplementary Information

Seasonality and reduced nitric oxide titration dominated ozone increase during COVID-19 lockdown in eastern China

Hongli Wang[a,1], Cheng Huang[a,1,2], Wei Tao[b,1], Yaqin Gao[a], Siwen Wang[b], Shengao Jing[a], Wenjie Wang[b], Rusha Yan[a], Qian Wang[a], Jingyu An[a], Junjie Tian[a], Qingyao Hu[a], Shengrong Lou[a], Ulrich Pöschl[b], Yafang Cheng[c,2], Hang Su[a,b,2]

[a], State Environmental Protection Key Laboratory of Formation and Prevention of Urban Air Pollution Complex, Shanghai Academy of Environmental Sciences, Shanghai 200233, China

[b], Multiphase Chemistry Department, Max Planck Institute for Chemistry, Mainz 55128, Germany

[c], Minerva Research Group, Max Planck Institute for Chemistry, Mainz 55128, Germany

[1], These authors contributed equally to this work.

[2], Corresponding author: h.su@mpic.de (H.S.); yafang.cheng@mpic.de; (Y.C.) huangc@saes.sh.cn (C.H.)

This PDF file includes:

Supplementary Figures 1 to 17
Supplementary Tables 1 to 5
Supplementary References

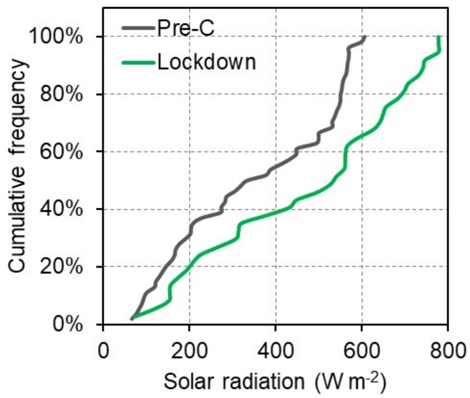

Supplementary Figure 1. The cumulative frequency of the daily maximum solar radiation before and during lockdown period in YRD region. Data were same to those in Figure 1.

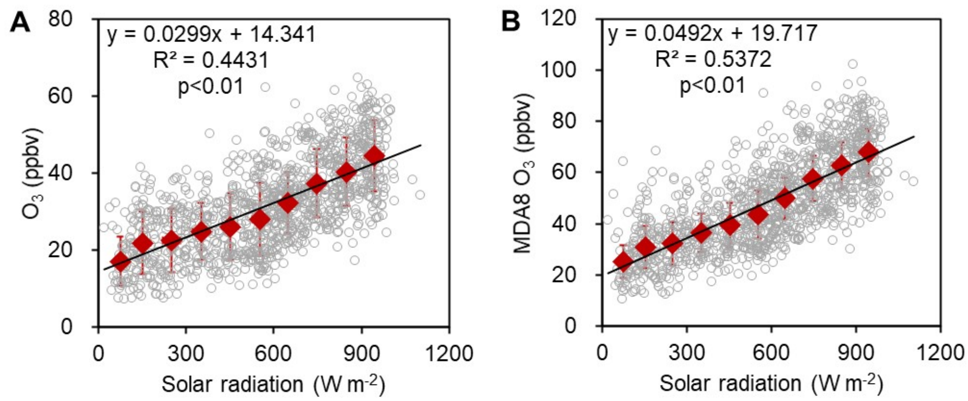

Supplementary Figure 2. Scatter plot of daily average of O_3 (A) and MDA8 O_3 (B) with daily maximum of solar radiation in YRD region from 2017 to 2019. The red marker indicated the average of each bin of solar radiation (0~100, 100~200, 200~300, 300~400, 400~500, 500~600, 600~700, 700~800, 800~900, >900), and the bars over the markers were the standard variations of data in each bin. The black line was the linear fitting of the daily data. Data were similar to those in Figure 1 but from 2017 to 2019. According to the fitting formula, the increase of O_3 during lockdown period compared to that before can be estimated primarily combined with the difference of solar radiation before and during lockdown periods, which may explain 24% of O_3 increase during lockdown period.

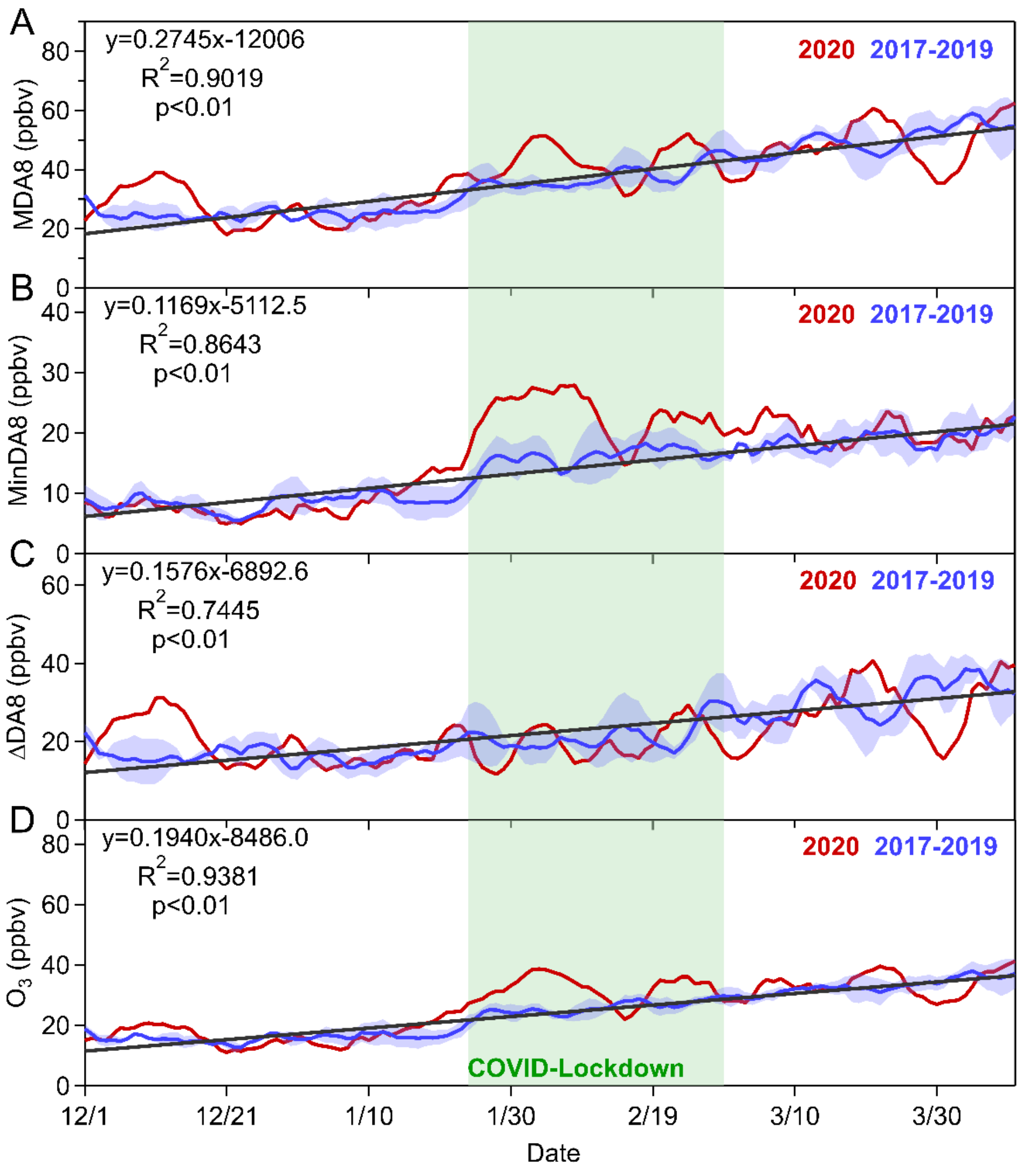

Supplementary Figure 3. Interannual comparisons of ozone variations before, during and after the COVID-19 lockdown in YRD region from 2017 to 2020. Values in 2020 (red lines in panel a-d) were same to Figure1 but extended to 10th April. The blue lines similar to red lines but for 2017 to 2019, and the blue shade was the interannual variations. The black lines were the linear regressions of data in 2017-2019, which represented the "normal" trend of ozone variations during these months. This "normal trend" was the combining result of enhancement of background and the meteorology fluctuation during the seasonal alternation. Panel A-D presented the time series of 5-day moving averages of MDA8 O_3, MinDA8 O_3, ΔDA8 O_3, and O_3 from top to bottom, respectively. According to the fitting formula, the increase of O_3 due to the seasonal variation can be estimated primarily, which may explain 58% of O_3 increase during lockdown period.

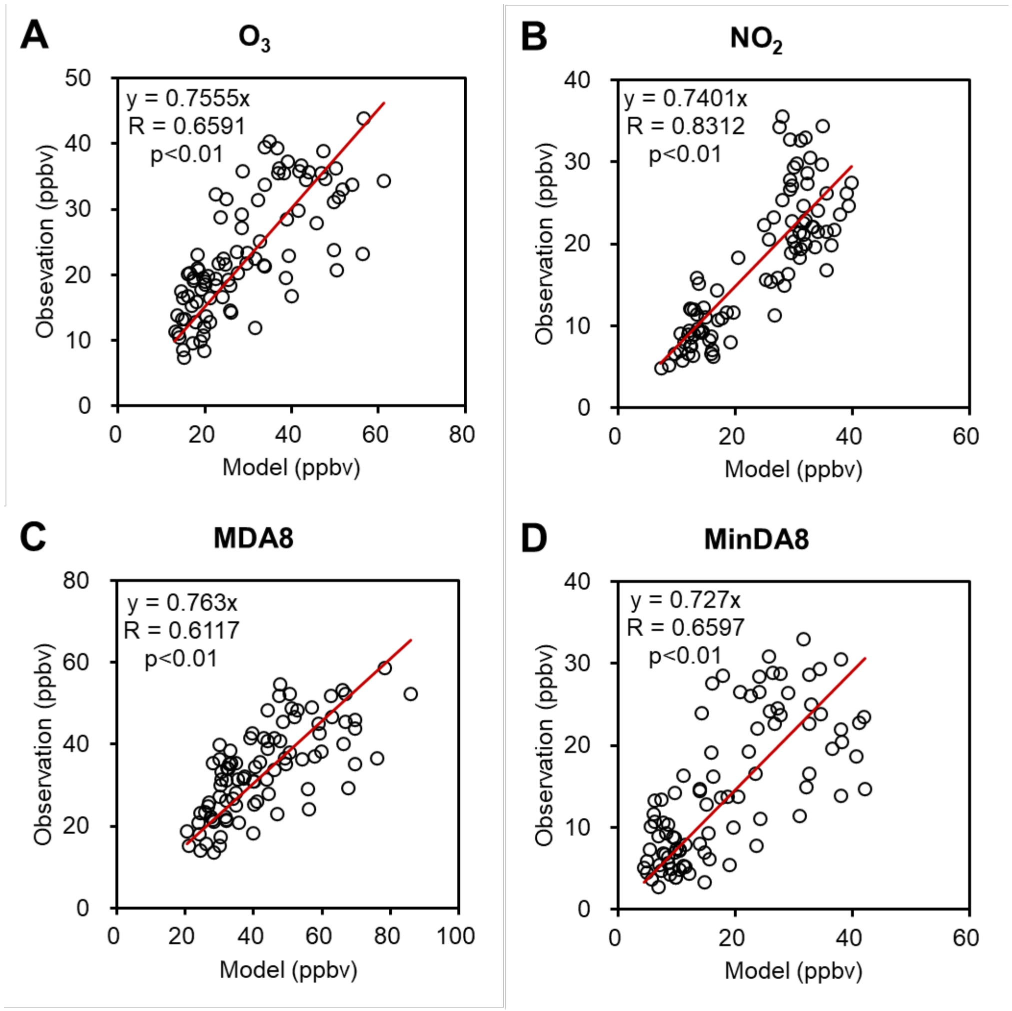

Supplementary Figure 4. Evaluations of model simulations with ambient measurements in YRD region. The observed data were same to Figure 1, and the model simulations were from COVID case. Panel A-D, Scatter plot of simulations verse observations for daily O_3, daily NO_2, MDA8 O_3, and MinDA8 O_3 before and during lockdown periods, respectively.

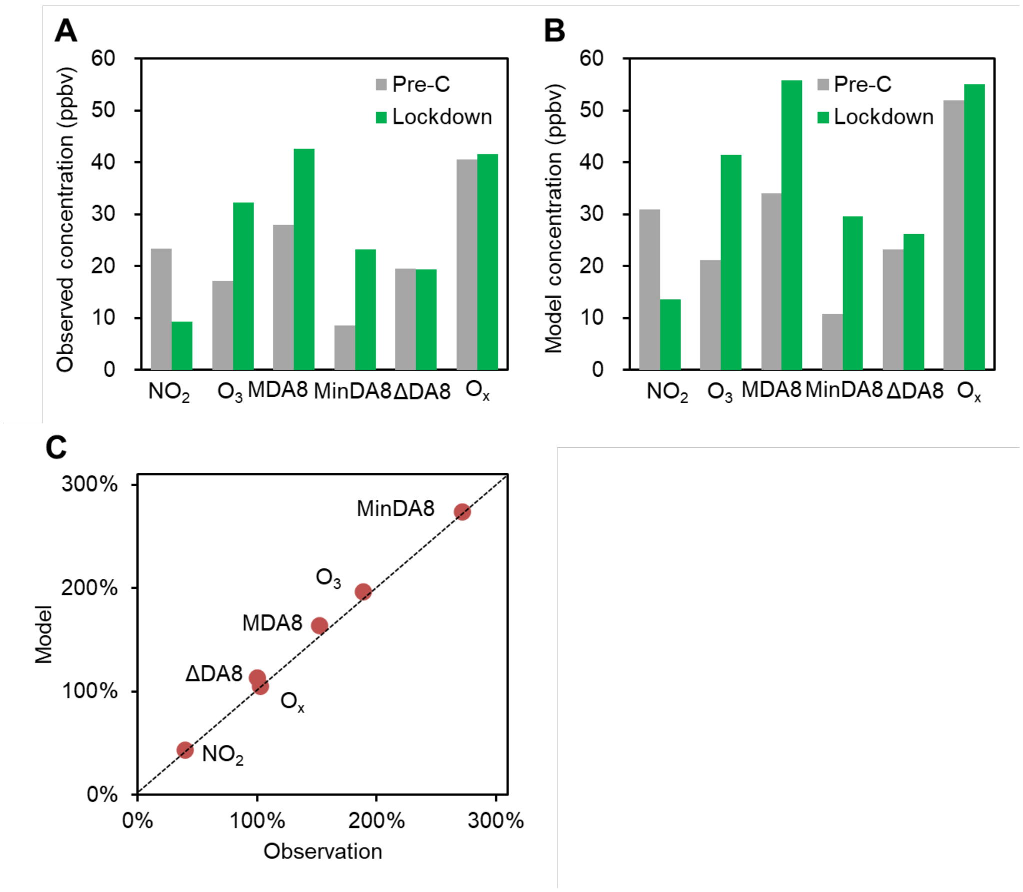

Supplementary Figure 5. Changes of ozone and NO_2 before and during lockdown period in YRD region. Panel A, Observation based results. Panel B, Model simulations based results. Panel C, Scatter plot of the observed and model simulation based results. The x and y axis indicated the observed and model simulated ratios of concentration during lockdown to that before lockdown. The dashed line indicated 1:1. As shown, the present model could well capture the changes of ozone and NO_2 before and during lockdown in YRD region.

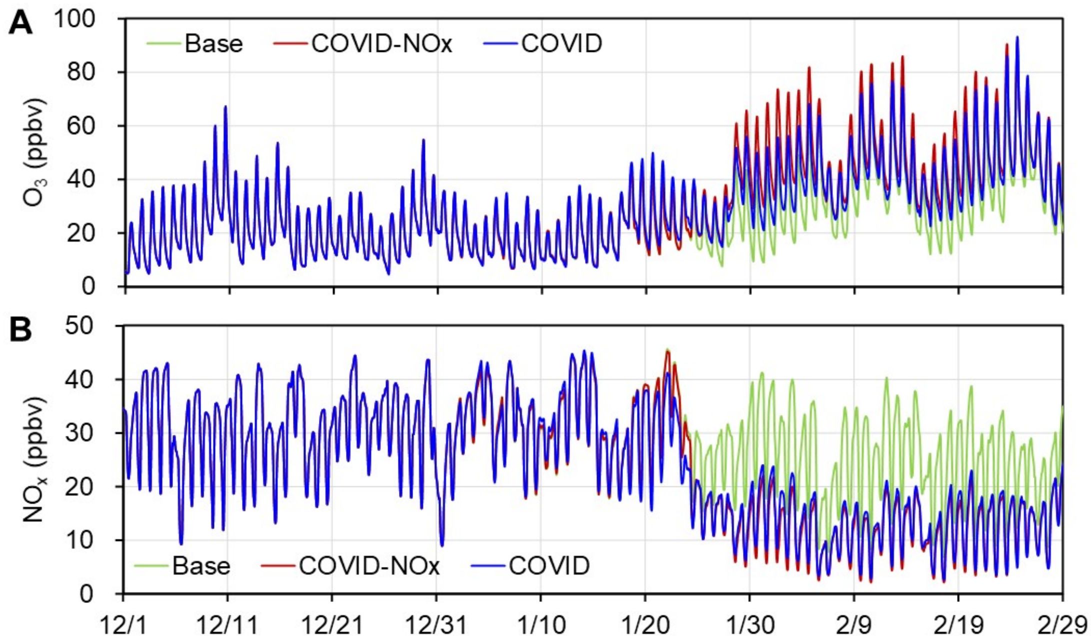

Supplementary Figure 6. Comparisons of the simulations from different case in YRD region. Base, simulation with fixed emissions as those before lockdown; COVID, simulation with the real emissions considering the lockdown emissions; COVID-NO_x, similar COVID case but without VOCs reductions during lockdown. Panel A-B, Time series of O_3 and NO_x from three simulations, respectively.

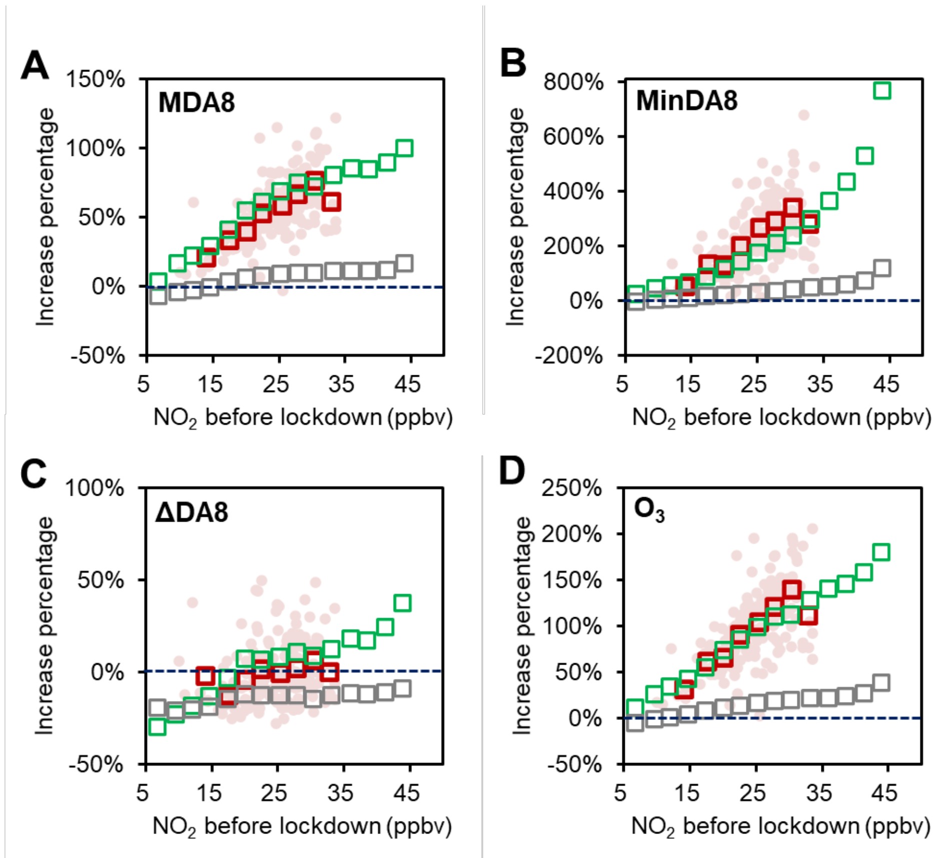

Supplementary Figure 7. Dependence of ozone changes before and during lockdown on NO_2 concentrations in YRD region. The x axis was NO_2 concentrations before lockdown, which indicated the present status of NO_2 pollution in YRD region. The y axis was calculated by the differences of ozone concentrations before and during lockdown. The red markers indicated the measured results. The green markers indicated the model simulated results in COVID case. The light dots were the data at the monitoring sites (190 sites in YRD region). The squares (red) were the averages over 2.5 ppbv NO_2 bins for data in different sites, and data below 15ppbv (only 6 data) were grouped together; all of the squares except the first and last one were grouped by more than 15 points, and uncertainties of the first (6 points) and last (8 points) squares were relatively higher due to few data points. The green squares were similar to those red but with the model simulated data from all the grids (862 grids) over YRD domain. The grey squares were the simulated results but corrected by the meteorology through the differences of ozone simulations in Base case before and during lockdown. Panel A-D, were MDA8 O_3, MinDA8 O_3, ΔDA8 O_3, and O_3, respectively.

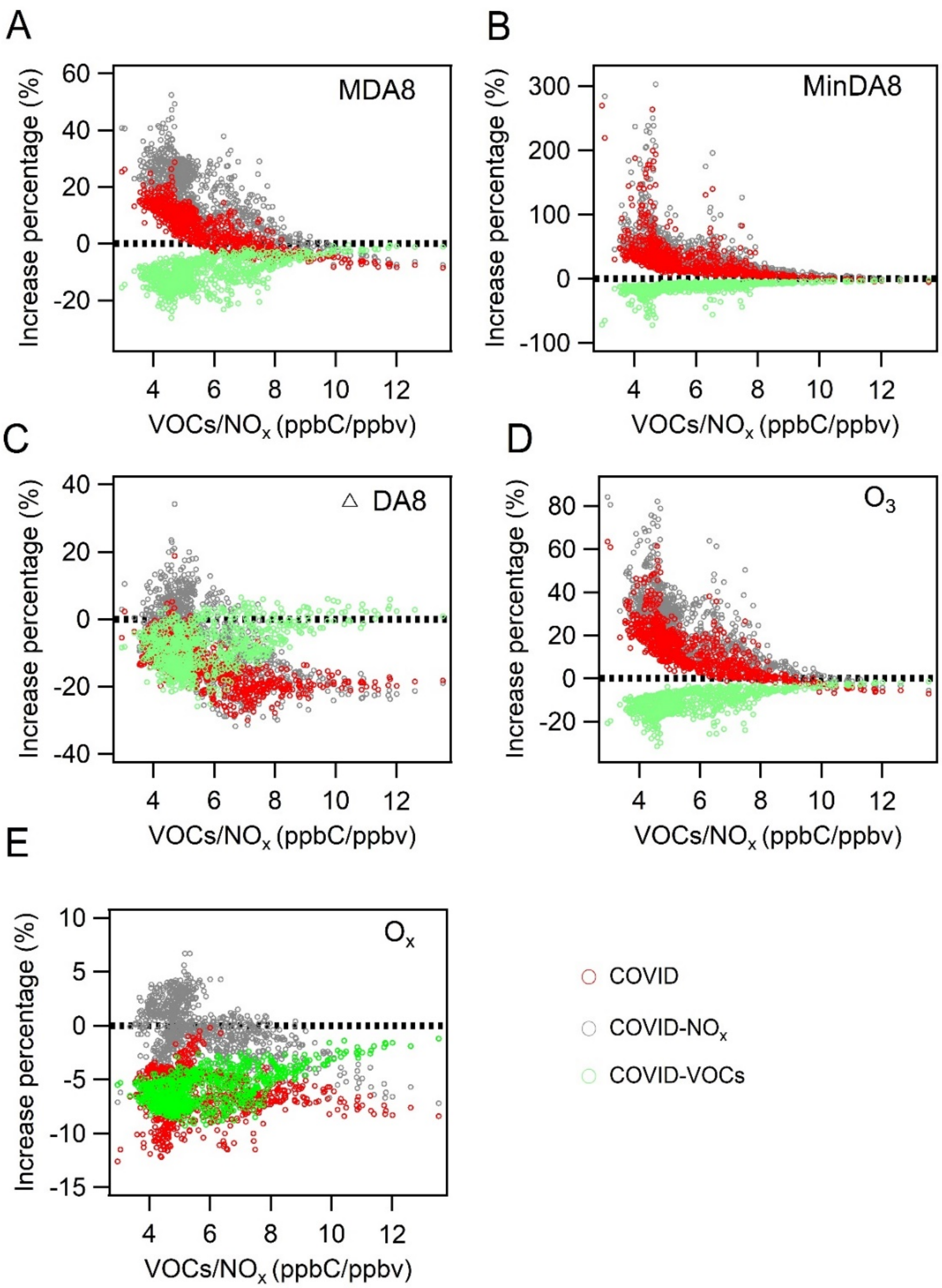

Supplementary Figure 8. Dependence of ozone changes on the ratios of VOCs to NO_x in different cases in the YRD region. Data were from the model simulations in Base, COVID, and COVID-NO_x cases during lockdown period. The increase percentages indicated by y axis were calculated by ozone changes between control case and Base case. Here, the difference between the COVID and COVID-NO_x simulated results was defined as COVID-VOCs case which indicated the impact of VOCs reductions on ozone. The x axis was the ratios of VOCs to NO_x from Base case during lockdown period. The markers were the data in different grids. Panel A-E, were MDA8 O_3, MinDA8 O_3, ΔDA8 O_3, O_3, and O_x, respectively.

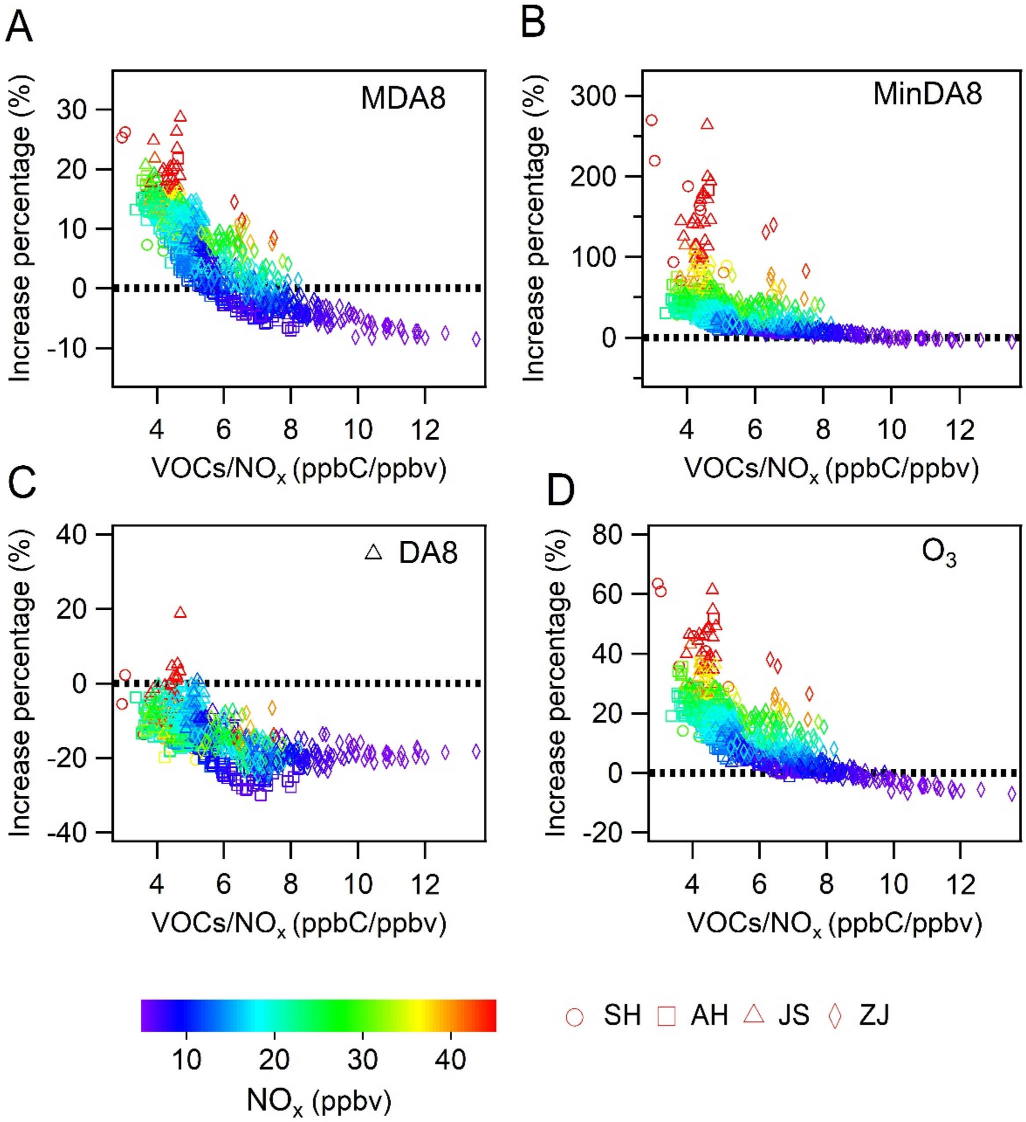

Supplementary Figure 9. Dependence of changes of ozone on ratios of VOCs/NO_x in the YRD region. Data were same as Figure 4. The markers were the data in different grids. The color represented the simulated NO_x concentrations in Base case. Panel A-D, were MDA8 O_3, MinDA8 O_3, ΔDA8 O_3, and O_3, respectively. SH, Shanghai; AH, Anhui province; JS, Jiangsu province; ZJ, Zhejiang province.

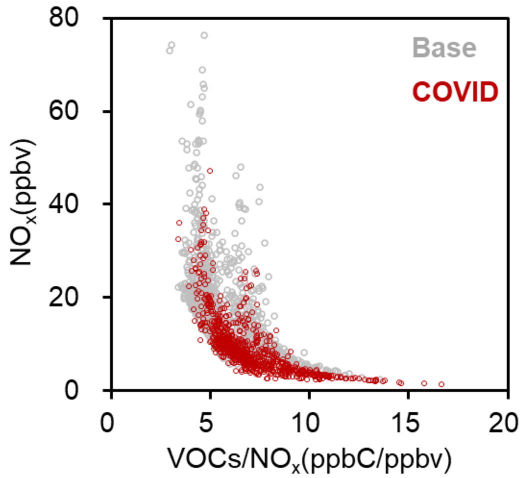

Supplementary Figure 10. Scatter plot of VOCs/NO_x ratios with NO_x concentrations. Values were from model simulations during lockdown period. Each marker indicated the data in each grid. The gray cycles were from the Base case, and the red ones from the COVID case. This high correlation between VOCs/NO_x ratios with NO_x concentrations suggested the ratios were largely depended on NO_x concentrations in YRD region.

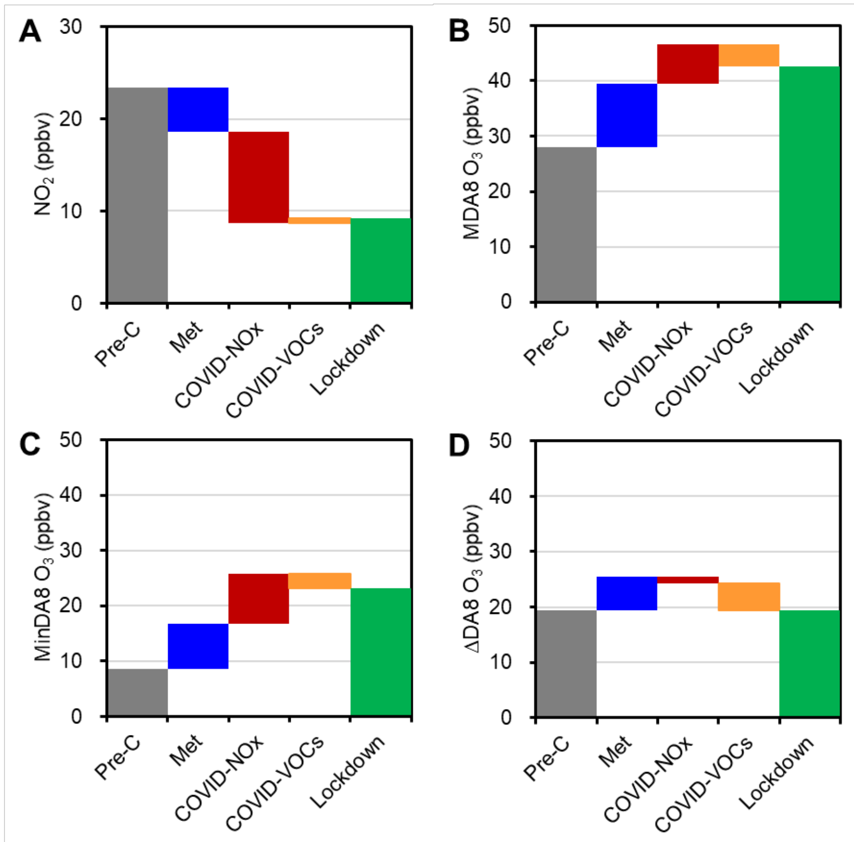

140 **Supplementary Figure 11.** Impacts of COVID-19 lockdown and meteorology on NO_2 and ozone related parameters in YRD region. Similar to Figure 2. But for A, the average NO_2. B, MDA8 O_3. C, MinDA8 O_3, and D, ΔDA8 O_3.

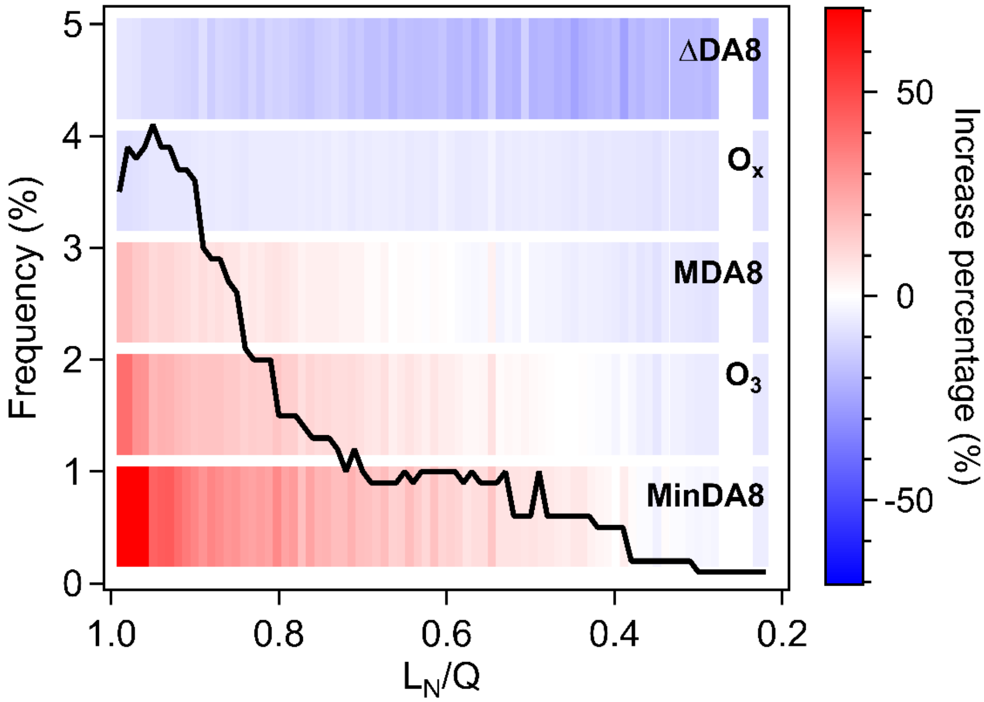

Supplementary Figure 12. Dependence of changes of ozone with and without lockdown reductions on L_N/Q. The x axis was the simulated L_N/Q in each grid from Base case grouped over 0.01 L_N/Q bins, which indicated the present status in YRD region. There were 862 grids in YRD domain in the model. The horizontal bar presented the dependence of changes of ozone between the Base and COVID cases during lockdown period on VOCs/NO_x ratios (those from Base case during lockdown), with the color bar axis as well as the x axis, and the blank areas indicated no data samples under these ratios. The lines were the frequency of different L_N/Q from Base case indicated by the y and x arises. The L_N/Q was the fraction of free radicals which are removed by reacting with NO_x.

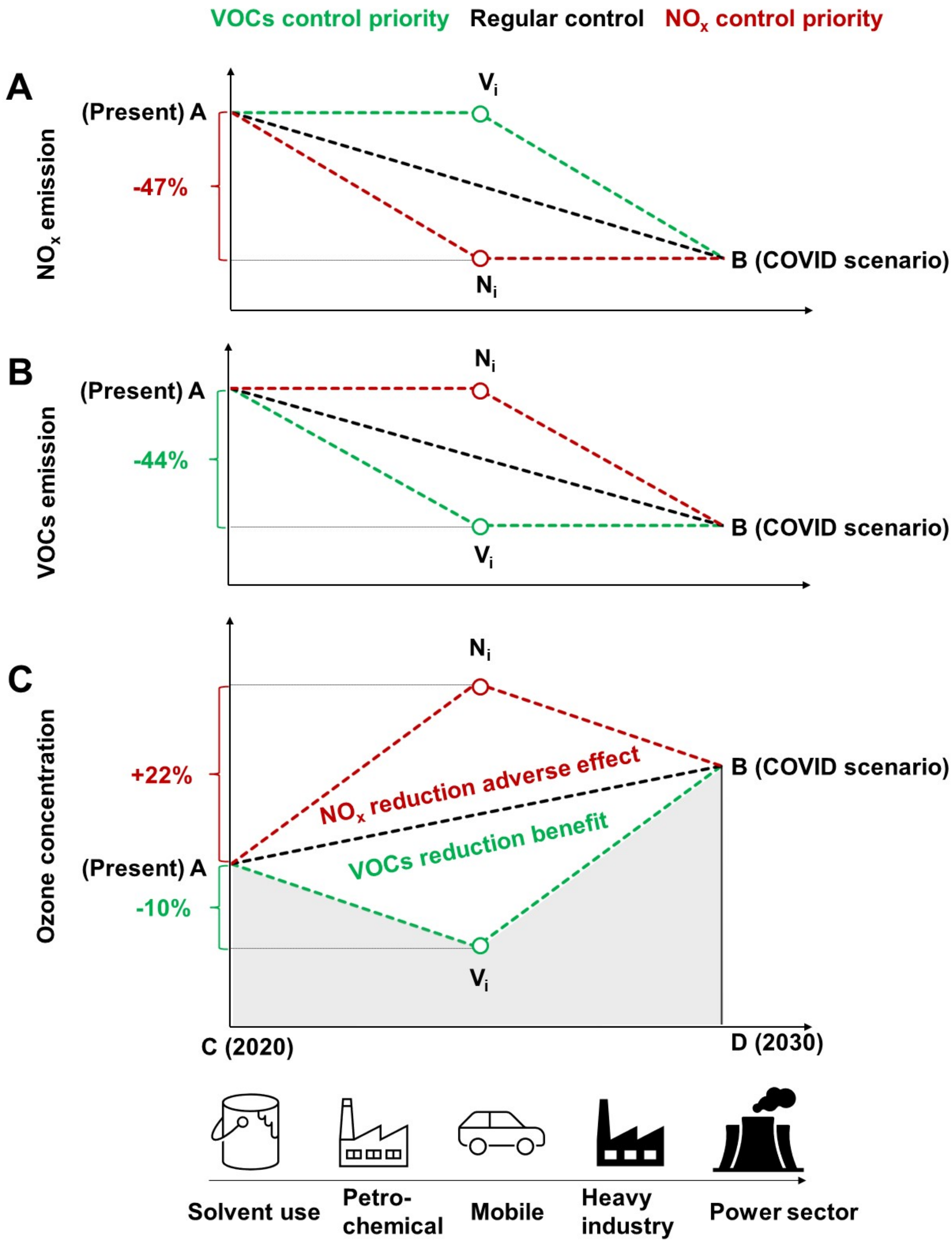

Supplementary Figure 13. Evolution of ozone concentrations under different timetable of precursors reductions in the winter/spring of the YRD region. Panel A, timetable of NO_x reduction; B, timetable of VOCs reduction; C, evolution of O_3 concentration corresponds to different timetable of precursors reductions. A, indicates the present status of O_3 concentration and precursors emissions, which in 2030 (denoted as B) are obtained assuming the same final emission control target in 2030 as that of COVID lockdown, which is still beyond the VOCs/NO_x emission reduction under a strong low-carbon policy and air pollution control policy[1]. There are three paths from A to B, including black dash line (A→B), red dash line (A→N_i→B), and green dash line (A→V_i→B), which correspond to different timetable of precursor emission reduction, namely regular control, NO_x control priority, and VOCs control priority, respectively. In panel C, the shadow area of the polygon AXBDC ($X=V_i/N_i$, correspond to VOCs/NO_x control priority) indicates the 10-year average O_3 concentration, compared to that of quadrangle ABDC under the regular control. The ideal path results in a lowest 10-year average O_3 concentration, which means the shadow area of the polygon AXBDC is minimum. Apparently, when we postpone the NO_x reduction (green dash line), the 10-year average O_3 would decrease, and vice versa. Thus, we may benefit more from a relatively slow reduction of NO_x in the beginning. Considering the different emissions ratios of VOCs/NO_x from various sources, sources mainly emitting VOCs but few NO_x, such as solvent usage and petrochemical industry[2] should be given more priority to.

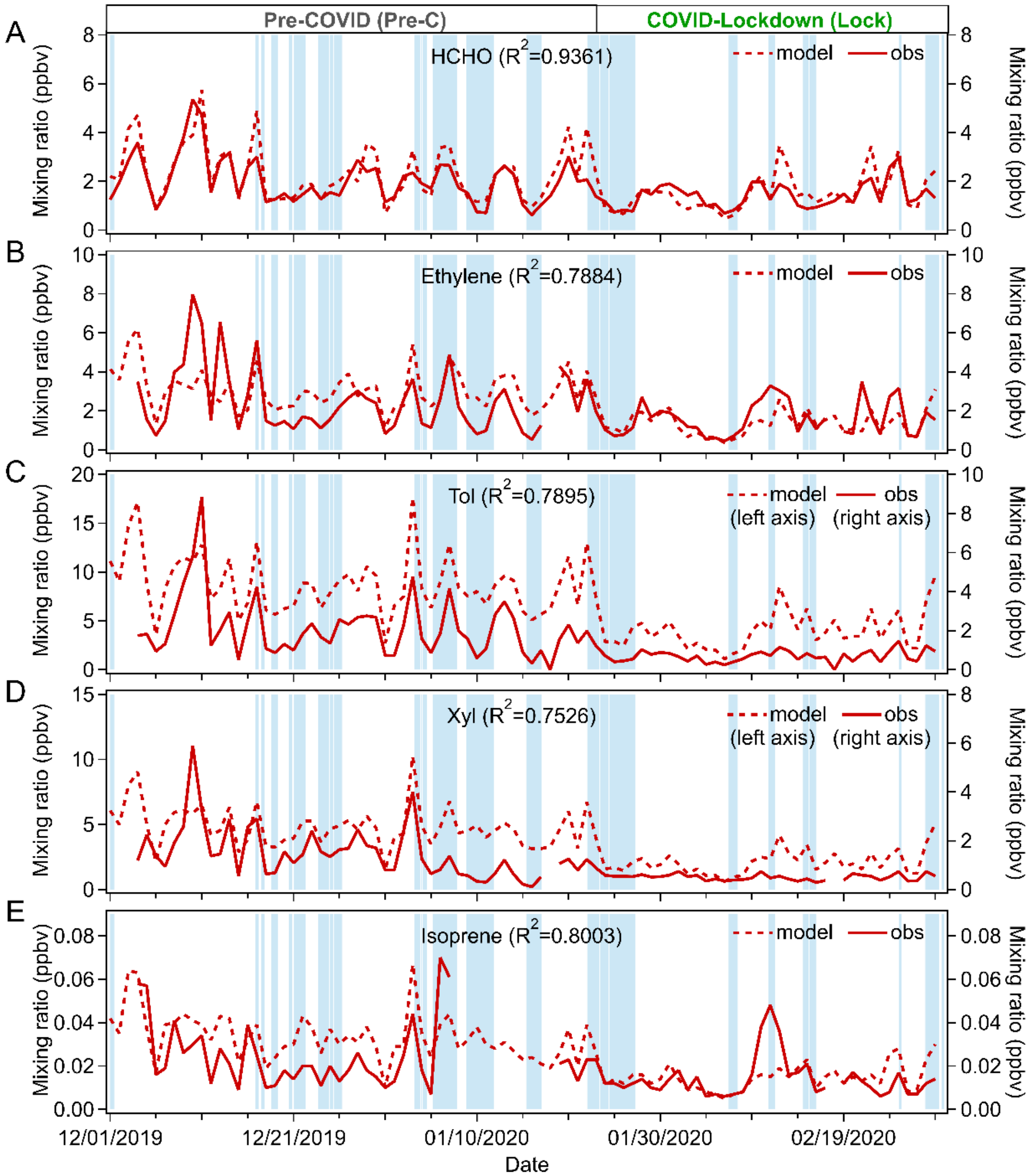

Supplementary Figure 14. Evaluations of model simulations of temporal variations of VOCs with field observations in Shanghai. The observed data were results at the campus of the Shanghai Academy of Environmental Sciences in Shanghai. Tol indicated the lump of toluene and less reactive aromatics in model simulations[3], and accordingly the observed Tol here was the sum of toluene, benzene and ethylbenzene. Similarly, Xyl in model simulations indicated the lump of xylene and more reactive aromatics[3], and the observed Xyl here was the sum of m,p,o-xylenes, styrene, C9 i,n-propylbenzenes, Trimethylbenzenes, m,p,o-ethyltoluenes) and C10 (m,p-diethylbenzenes) aromatics here.

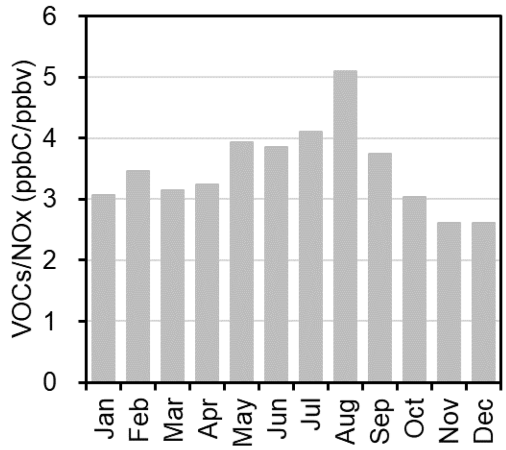

Supplementary Figure 15. Monthly pattern of the ratio of VOCs to NO_x in a Shanghai megacity located in eastern YRD. Data were from the measurements in SAES supersite in Shanghai located in eastern YRD in 2019. VOCs included 56 kinds of non-methane hydrocarbons.

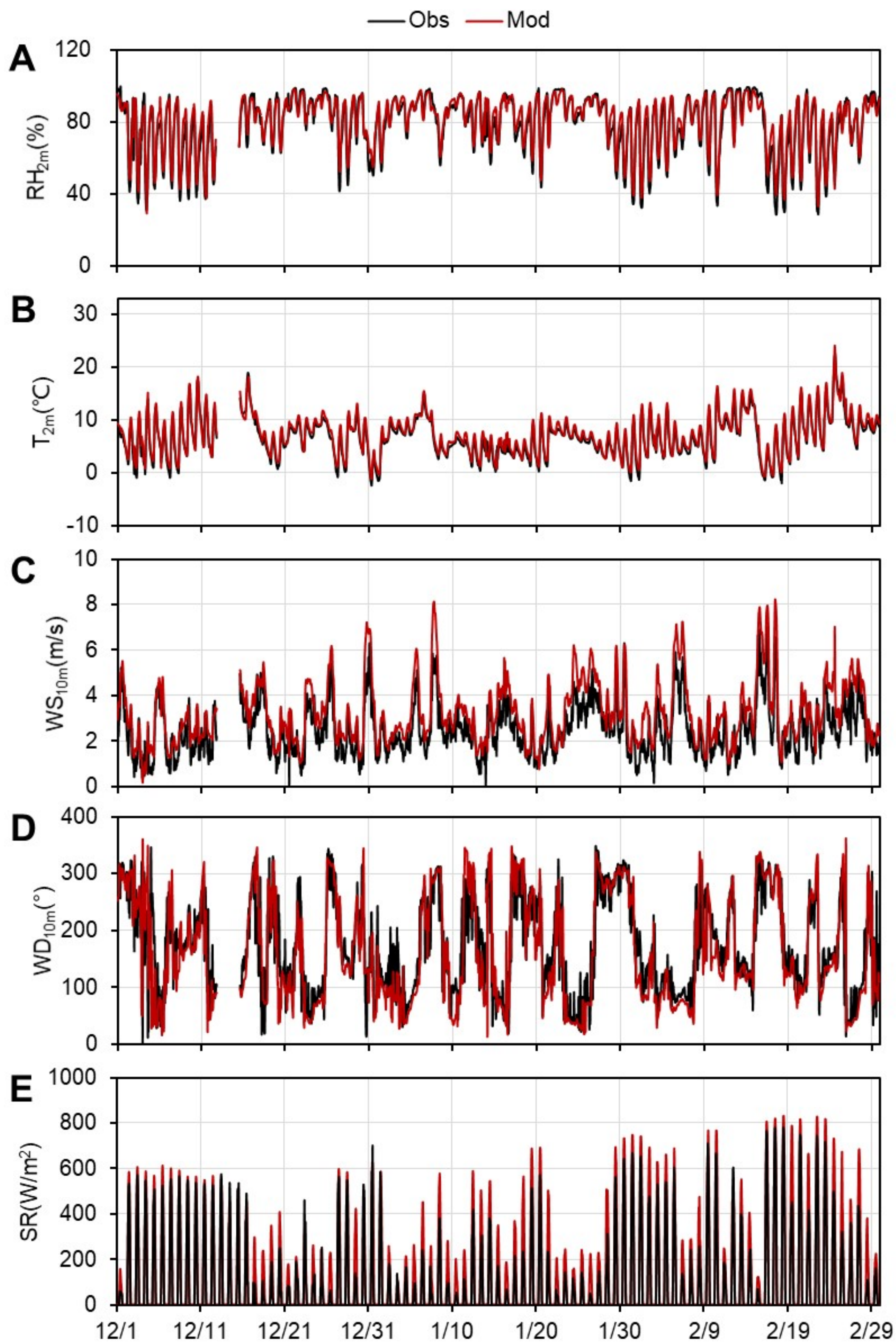

Supplementary Figure 16. Evaluations of model simulations of temporal variations of meteorology with field observations in YRD region. The observed data (black lines) were the average results at 5 sites in 5 cities in YRD region from the national meteorological observing stations operated by the China Meteorological Administration. Panels A-E indicate 2-m relative humidity, 2-m temperature, 10-m wind speed and direction, and solar radiation.

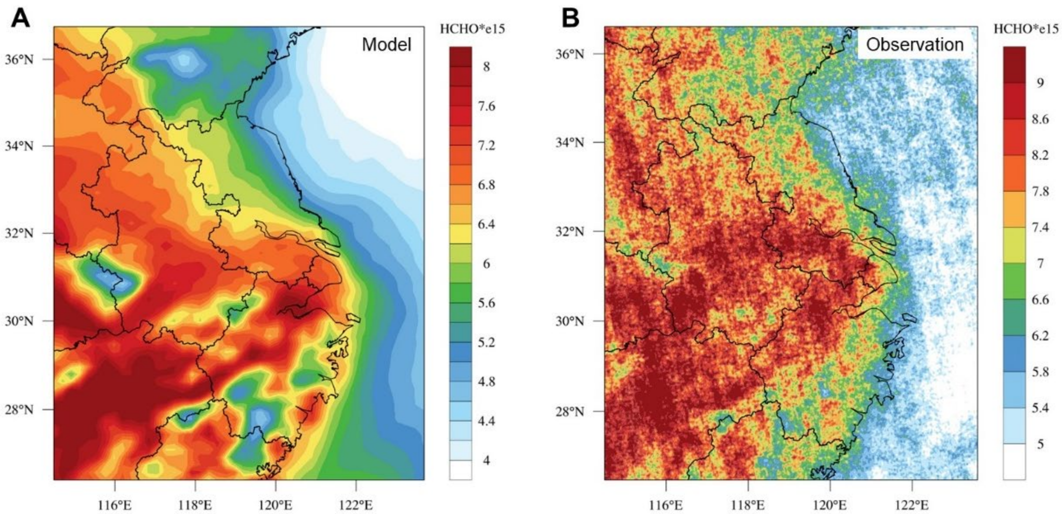

Supplementary Figure 17. Spatial distribution of formaldehyde column densities. Data were the average during lockdown period. Panel A, the model simulations with a resolution of 20 km; panel B, the measurements retrieved from OMPS at 3.5 km resolution[4].

Supplementary Table 1. NO_x and VOCs emissions and their emission ratio in different sectors in YRD region. Dada were from our previous study[2]. Here, heavy industry includes coking, iron and steel, and cement production; mobile sources include on/off-road vehicles, ships and aircraft; petro-chemical industry includes petroleum refining, chemical material production, and glass production. Solvent usage mainly includes coating, printing, textile, etc.

	NO_x (ton/day)	VOCs (ton/day)	NO_x/VOCs (ton/ton)
Power sector	1223	33	37.0
Heavy industry	1210	137	8.8
Mobile	4586	2372	1.9
Petro-chemical industry	617	3107	0.2
Solvent usage	163	2714	0.1
Others	552	3567	0.2

Supplementary Table 2. Correlation (R) of observations and simulations on a spatial scale

City	daily NO_2	daily O_3	MDA8 O_3	MinDA8 O_3	ΔDA8 O_3
75th percentile	**0.788**	**0.703**	**0.659**	**0.651**	**0.462**
median	**0.723**	**0.662**	**0.631**	**0.614**	**0.406**
25th percentile	**0.632**	**0.602**	**0.561**	**0.501**	**0.338**
Anqing	0.37	0.57	0.66	0.28	0.37
Bengbu	0.78	0.70	0.66	0.62	0.53
Bozhou	0.79	0.69	0.64	0.62	0.27
Changzhou	0.78	0.70	0.63	0.65	0.42
Chizhou	0.54	0.60	0.57	0.47	0.25
Chuzhou	0.80	0.70	0.65	0.61	0.42
Fuyang	0.71	0.72	0.70	0.64	0.30
Hangzhou	0.78	0.64	0.63	0.61	0.52
Hefei	0.76	0.78	0.75	0.65	0.55
Huzhou	0.65	0.65	0.55	0.65	0.36
Huai'an	0.84	0.67	0.60	0.68	0.34
Huaibei	0.85	0.73	0.70	0.71	0.41
Huainan	0.78	0.72	0.70	0.69	0.61
Huangshan	0.58	0.37	0.48	-0.04	-0.01
Jiaxing	0.72	0.74	0.65	0.68	0.43
Jinhua	0.50	0.55	0.52	0.50	0.44
Lishui	0.44	0.54	0.55	0.36	0.21
Lianyungang	0.77	0.69	0.60	0.69	0.28
Lu'an	0.58	0.69	0.69	0.56	0.39
Maanshan	0.69	0.60	0.59	0.50	0.34
Nanjing	0.79	0.67	0.70	0.49	0.43
Nantong	0.87	0.66	0.55	0.67	0.46
Ningbo	0.71	0.75	0.64	0.70	0.37
Quzhou	0.54	0.56	0.54	0.46	0.21
Shanghai	0.78	0.81	0.75	0.76	0.57
Shaoxing	0.71	0.65	0.61	0.58	0.48
Suzhou	0.79	0.70	0.64	0.60	0.43
Taizhou(ZJ)	0.62	0.60	0.60	0.55	0.37
Taizhou(JS)	0.86	0.63	0.50	0.64	0.40
Tongling	0.45	0.35	0.45	0.20	0.37
Wenzhou	0.72	0.71	0.63	0.75	0.51
Wuxi	0.80	0.69	0.64	0.60	0.43
Wuhu	0.69	0.62	0.63	0.53	0.59
Suqian	0.70	0.62	0.66	0.57	0.44
Suzhou	0.72	0.65	0.64	0.62	0.37
Xvzhou	0.79	0.73	0.75	0.62	0.46
Xuancheng	0.64	0.57	0.61	0.47	0.27
Yancheng	0.82	0.63	0.46	0.62	0.39
Yangzhou	0.87	0.69	0.63	0.64	0.45
Zhenjiang	0.78	0.66	0.65	0.54	0.47
Zhoushan	0.52	0.46	0.34	0.50	0.14

Supplementary Table 3. Normalized mean bias (NMB) of observations and simulations on a spatial scale

City	daily NO_2	daily O_3	MDA8 O_3	MinDA8 O_3	ΔDA8 O_3
75th percentile	57%	39%	38%	50%	-1%
median	33%	24%	23%	18%	-8%
25th percentile	1%	7%	9%	2%	-20%
Anqing	-2%	16%	16%	18%	-23%
Bengbu	1%	31%	29%	36%	-15%
Bozhou	30%	24%	14%	45%	-32%
Changzhou	61%	-6%	8%	-26%	-5%
Chizhou	-6%	95%	76%	133%	-1%
Chuzhou	0%	18%	23%	11%	-10%
Fuyang	17%	39%	30%	52%	-20%
Hangzhou	76%	32%	45%	6%	25%
Hefei	34%	29%	38%	21%	3%
Huzhou	30%	37%	33%	38%	-3%
Huai'an	39%	13%	17%	6%	-12%
Huaibei	55%	3%	6%	2%	-21%
Huainan	33%	17%	23%	12%	-11%
Huangshan	2%	67%	40%	111%	-37%
Jiaxing	54%	17%	25%	8%	-3%
Jinhua	-14%	128%	93%	196%	1%
Lishui	-22%	120%	81%	209%	-19%
Lianyungang	-10%	34%	22%	58%	-36%
Lu'an	-3%	39%	33%	49%	-17%
Maanshan	35%	41%	40%	50%	-3%
Nanjing	65%	-17%	2%	-45%	-2%
Nantong	85%	-9%	6%	-29%	-1%
Ningbo	53%	11%	16%	6%	-8%
Quzhou	-19%	100%	80%	132%	0%
Shanghai	52%	-7%	6%	-24%	-6%
Shaoxing	75%	32%	42%	13%	15%
Suzhou	107%	-27%	-2%	-64%	-1%
Taizhou(ZJ)	36%	40%	36%	49%	-12%
Taizhou(JS)	59%	8%	10%	2%	-16%
Tongling	11%	33%	37%	26%	3%
Wenzhou	26%	58%	52%	64%	10%
Wuxi	97%	-18%	4%	-50%	0%
Wuhu	42%	23%	27%	19%	-9%
Suqian	8%	25%	16%	40%	-32%
Suzhou	13%	27%	19%	41%	-24%
Xvzhou	44%	8%	7%	15%	-24%
Xuancheng	14%	9%	17%	-2%	-3%
Yancheng	19%	6%	1%	13%	-38%
Yangzhou	77%	-5%	8%	-28%	-7%
Zhenjiang	79%	0%	13%	-20%	-4%

Zhoushan	-15%	41%	32%	55%	-31%

Supplementary Table 4. Normalized mean error (NME) of observations and simulations on a spatial scale

City	daily NO_2	daily O_3	MDA8 O_3	MinDA8 O_3	ΔDA8 O_3
75th percentile	59%	51%	46%	71%	43%
median	48%	39%	34%	65%	38%
25th percentile	40%	36%	30%	54%	36%
Anqing	52%	39%	29%	65%	46%
Bengbu	27%	41%	37%	56%	35%
Bozhou	41%	38%	31%	71%	39%
Changzhou	63%	36%	34%	58%	37%
Chizhou	44%	101%	80%	151%	49%
Chuzhou	28%	35%	34%	52%	37%
Fuyang	36%	47%	39%	73%	38%
Hangzhou	76%	52%	55%	62%	46%
Hefei	40%	44%	45%	62%	33%
Huzhou	46%	49%	45%	67%	43%
Huai'an	42%	30%	29%	39%	37%
Huaibei	55%	32%	27%	52%	35%
Huainan	39%	36%	35%	50%	30%
Huangshan	53%	74%	47%	131%	59%
Jiaxing	59%	36%	37%	55%	38%
Jinhua	39%	132%	96%	205%	43%
Lishui	50%	121%	81%	214%	48%
Lianyungang	29%	39%	30%	69%	41%
Lu'an	42%	45%	39%	65%	42%
Maanshan	45%	58%	49%	92%	39%
Nanjing	66%	39%	31%	67%	38%
Nantong	86%	29%	26%	48%	37%
Ningbo	56%	31%	30%	48%	35%
Quzhou	40%	103%	81%	138%	50%
Shanghai	54%	28%	24%	47%	33%
Shaoxing	77%	51%	51%	67%	40%
Suzhou	107%	38%	33%	71%	42%
Taizhou(ZJ)	56%	49%	41%	69%	39%
Taizhou(JS)	60%	30%	30%	44%	38%
Tongling	43%	57%	52%	78%	42%
Wenzhou	48%	61%	55%	71%	38%
Wuxi	97%	37%	34%	67%	38%
Wuhu	49%	51%	43%	79%	35%
Suqian	33%	37%	27%	62%	38%
Suzhou	36%	39%	30%	60%	37%
Xvzhou	47%	36%	28%	65%	35%

Xuancheng	42%	36%	33%	47%	44%
Yancheng	35%	27%	24%	44%	44%
Yangzhou	77%	34%	31%	55%	34%
Zhenjiang	81%	36%	33%	62%	35%
Zhoushan	52%	45%	37%	60%	53%

Supplementary Table 5. The model performance in simulating ozone and NO_2

	daily NO_2	daily O_3	MDA8 O_3	MinDA8 O_3	Criteria[4]
NMB[1]	0.353	0.259	0.263	0.271	<0.15
NME[2]	0.384	0.328	0.306	0.442	<0.25
IOA[3]	0.772	0.743	0.697	0.773	/
R	0.831	0.659	0.611	0.660	>0.50

[1] NMB is normalized mean bias, $NMB = \frac{\sum_{i=1}^{N}(C_m - C_0)}{\sum_{i=1}^{N} C_0} \times 100\%$, C_m represents simulated value, C_0 represents observed value, the same below.

[2] NME is normalized mean error, $NME = \frac{\sum_{i=1}^{N}|C_m - C_0|}{\sum_{i=1}^{N} C_0} \times 100\%$

[3] IOA is index of agreement, $IOA = 1 - \frac{\sum_{i=1}^{N}(C_m - C_o)^2}{\sum_{i=1}^{n}(|C_0 - \overline{C_0}| + |C_m - \overline{C_m}|)^2}$

[4] Emery et al., 2016[5]

Supplementary References.

1. Tong, D. *et al.* Dynamic projection of anthropogenic emissions in China: methodology and 2015–2050 emission pathways under a range of socio-economic, climate policy, and pollution control scenarios. *Atmospheric Chemistry and Physics* **20**, 5729-5757, doi:10.5194/acp-20-5729-2020 (2020).
2. An, J. *et al.* Emission inventory of air pollutants and chemical speciation for specific anthropogenic sources based on local measurements in the Yangtze River Delta region, China. *Atmospheric Chemistry and Physics* **21**, 2003-2025, doi:10.5194/acp-21-2003-2021 (2021).
3. Stockwell, W. R., Kirchner, F., Kuhn, M. & Seefeld, S. A new mechanism for regional atmospheric chemistry modeling. *Journal of Geophysical Research: Atmospheres* **102**, 25847-25879, doi:10.1029/97jd00849 (1997).
4. Su, W. *et al.* Primary and secondary sources of ambient formaldehyde in the Yangtze River Delta based on Ozone Mapping and Profiler Suite (OMPS) observations. *Atmospheric Chemistry and Physics* **19**, 6717-6736, doi:10.5194/acp-19-6717-2019 (2019).
5. Emery, C. *et al.* Recommendations on Statistics and Benchmarks to Assess Photochemical Model Performance. *J Air Waste Manag Assoc*, doi:10.1080/10962247.2016.1265027 (2016).